



Numerical Simulation of Thermal Storage Tank with Middle Baffles Distributions

Saad Sabah Karam¹, Sahira Hasan Ibrahim², Israa Alesbe², Sattar Aljabair^{2*}

¹ Department of Air Conditioning Engineering Technologies, Nukhba University College, Baghdad 10011, Iraq

² Mechanical Engineering Department, University of Technology-Iraq, Baghdad 10011, Iraq

Corresponding Author Email: sattar.j.aljabair@uotechnology.edu.iq

<https://doi.org/10.18280/mmep.100522>

ABSTRACT

Received: 31 January 2023

Revised: 30 April 2023

Accepted: 15 May 2023

Available online: 27 October 2023

Keywords:

thermal stratification, thermocline temperature, thermocline thickness, storage tank, CFD

A numerical investigation into the influence of baffle placement on thermal stratification within a vertical cylindrical cold-water tank is conducted. The tank, sporting a diameter of 400 mm and a height of 1000 mm, incorporates inlet and outlet ports of equal diameter (17.39 mm). The baffles, integral to this study, are of 200 mm in length and 2 mm in thickness. The study leverages computational methodologies to decipher the equations that govern heat transfer and fluid flow within a baffle-integrated tank. The tank commences with an initial water temperature of 4.4°C, and an inflow of water at 13.3°C, from the upper left side. Validation of the adopted tests is sought through experimental data available in extant literature. The abstract delves into the impact of baffle number and positioning on a multitude of elements—thermocline temperature, streamline creation, vortex formation, velocity vectors, Stratification Number, and Richardson Number—across varied cases during the discharging phase. The introduction of one or two baffles exerts a marginal effect on temperature distribution contours. However, a third baffle accentuates this impact, expanding the hot-cold interface with a pronounced penetration effect within the tank. Interestingly, the influence of three baffles on temperature distribution contours diminishes at a discharging time of 2173.4 s. This study provides insight into the nuanced role of baffles within thermal storage tanks, elucidating key considerations for their optimal placement and number.

1. INTRODUCTION

Solar hot water tanks, utilizing gravitational stratification to separate cold and hot water, are established energy-saving tools. A stratified tank, due to its simplicity and cost-effectiveness, is particularly suitable for low to medium operating temperatures. However, meeting diverse energy requirements, such as hot water, space heating, and air conditioning, necessitates higher storage tank temperatures [1]. An increasing number of researchers are investigating the performance of thermal storage systems, both numerically and experimentally [2-7]. The broad scope of thermal energy storage and its varied roles across different energy sources have been examined. Discussions have encompassed solar power production, building thermal comfort, and other specialized uses of thermal energy storage. Furthermore, in-depth reviews of thermal energy storage materials have been conducted, considering their properties, cost, operating performance, and applicability to specific requirements [8, 9].

The term "thermocline" denotes the mixing layer between cold and hot water, where the thickness of the thermocline becomes a critical parameter used to characterize thermal stratification. It has been previously established that within a highly stratified storage tank, the thermocline layer should be minimized [10]. Consequently, there has been a global surge in interest in thermal stratification in water tanks, with numerous numerical and experimental advancements reported in recent literature [11-17].

Preserving temperature stratification in liquid fluids is

crucial for the efficiency and proper operation of thermal collectors. Stratification mechanisms are influenced by operational flow rates, heat loss to the environment, mixing instigated by inlet and outlet fluids, tank designs, and discharging and charging passages [18]. Tesfay and Venkatesan [19] investigated various liquid medium thermal energy storage systems, and a mixed-media single-tank thermocline thermal energy storage was selected and built based on the Schumann equation. This equation was numerically solved to calculate energy storage at different locations and times within the storage tank. Shaikh et al. [20] examined the effect of several factors on thermocline thickness in solar home hot water systems, where hot water tanks are used to store hot water for future use. A porous medium flow distributor in the tank aids in reducing thermocline thickness. Vertical mantled hot water storage tanks are most common due to their ease of manufacture and superior thermal stratification.

Latent heat thermal energy storage is a promising method that enhances energy storage density [21]. The heat of fusion is stored isothermally at a temperature analogous to the phase-change temperature of the material.

Njoku et al. [22] conducted a review of numerical methods for modeling stratified thermal energy storage systems, assessing their strengths and weaknesses based on entropy and energy analyses. In a related study, Mao [23] evaluated the geometrical configuration of a thermal energy storage tank, providing valuable experimental and numerical references for the development, operation, and energy consumption

reduction of thermal energy storage systems, particularly in the context of solar plants.

The utility of Computational Fluid Dynamics (CFD) modeling was demonstrated by studies [24, 25] in their numerical investigation of three distinct shapes of thermal storage tanks: cylindrical tanks, circular truncated cone tanks, and spherical tanks. Of the three, the spherical tank resulted in the most symmetrical temperature stratification, while the truncated circular cone tank achieved superior temperature stratification and thermal charge efficiency.

Gao et al. [26] conducted experiments to examine the thermal stratification characteristics of a charging hot water storage tank equipped with a baffle plate. They identified baffle aperture and inlet velocity as significant interaction elements influencing the three indices. The response surface methodology was employed to optimize these structural parameters.

The sloshing phenomenon in rectangular and trapezoidal partially filled tanks was studied by studies [27, 28], utilizing the finite element method. Thirunavukkarasu and Rajagopal [29] performed a numerical analysis of the sloshing phenomena in a 3D square tank, focusing on resonant frequency and magnitude of stimulation. They measured and studied the liquid pressure within the container at regular intervals during stimulation. Baffles (both horizontal and vertical) and perforated obstacles emerged as preferred methods of controlling slosh force.

Sanapala et al. [30] utilized a baffle to examine the dynamics of sloshing under induced vertical harmonic excitations. After an extensive study of transient wave patterns, forces, and pressure time histories, they established the optimal baffle design. The optimal position and width of the baffle were systematically determined with reference to the quiescent free surface.

Boetcher et al. [31] investigated models of a water tank utilizing a heat exchanger within the tank, with the shroud and baffle being considered adiabatic and having parametrically changeable forms. This approach resulted in an increase in the temporal Nusselt number by up to twentyfold.

Finally, the potential of nanofluids as thermal storage mediums was highlighted, as they possess high thermal conductivity and heat capacity, enabling them to absorb and release heat more efficiently than traditional fluids [32, 33].

Goudarzi et al. [34] developed a methodology to determine the damping ratio of water sloshing for wall-bounded baffles, noting that the size and position of baffles significantly impacted hydrodynamic damping. The reliability of this theoretical approach was investigated, along with alternative baffle designs. The quantity of energy stored in the thermal tank and the duration of its storage were explored by studies [35, 36], who employed numerical modeling to conduct thermal and flow analyses with varying set temperature values. During the charging process, copper encapsulations displayed the highest temperature distribution from heat transfer fluid to phase change materials.

Gedikli et al. [37] scrutinized the effects of a stiff baffle on the seismic response of water in a cylindrical tank. A baffle, a structural element that passively mitigates the impacts of seismic movement, was found to be effective in controlling the flow, which was characterized as irrotational, incompressible, and viscous. The natural motions of liquid in a cylindrical tank were investigated using the boundary element approach.

Gualtieri [38] examined the thermal performance of indirect water storage tanks, employing a multiphase approach to

conduct two-dimensional steady-state and transient numerical simulations. One potential application of nanofluid-based thermal storage, involving both single and multiphase systems, is in solar thermal energy systems. These systems concentrate sunlight onto a fluid-filled receiver using mirrors or lenses; the heat energy thus absorbed is used to generate electricity or provide hot water. The use of nanofluid as the heat transfer fluid allows the system to operate at a higher efficiency and store excess heat energy for use when sunlight is unavailable [39-41].

A circular baffle configuration with a single intake and output yielded the highest Morrill Index score. Hashim and Abdulrasool [42] numerically investigated the impact of different types of curved baffles within a vertical hot storage tank, finding that type C baffles significantly increased thermal stratification at high flow rates due to their downward curvature shape, and thus provided the best thermal stratification.

Gao and Stenstrom [43] conducted an in-depth investigation of the effects of varying baffle dimensions on turbulence properties using decoupled/coupled SKE models. Stress tests were conducted where the dimensions partially mitigated the impact of buoyancy on turbulence, with the buoyancy-decoupled turbulence model providing qualitative yet similar predictions.

Alesbe et al. [44] reported on the thermal stratification of full-scale chilled water storage tanks during discharge mode under optimal conditions. The investigation involved a full-scale experimental and numerical analysis of a stratified thermal storage tank, with optimal operation conditions determined through numerous experiments. These conditions were characterized by high thermal stratification and minimal thermal mixing within the tank. The results included temperature stratification and flow parameters during operation, as well as thermal performance parameters such as discharge efficiency, Richardson number, stratification efficiency, thermocline thickness, average tank temperature, and discharge temperature.

The study's most significant outcome was the optimal stratification phenomena in the tank with limited thermal mixing. Experimental results for these phenomena were validated by numerical modeling and simulation settings, which also helped define the optimal conditions for thermal stratification, considering tank size, diffuser type, and flow rate.

The current work aims to analyze and improve the thermal stratification in a water thermal energy storage tank. This involves using three models of transferred baffle, each adding one, two, or three baffles, and analyzing the effect of these additions on various thermal and flow parameters. The simulation's objective is to understand the fluid behavior and temperature distribution within the tank.

2. PHYSICAL CASE STUDY

Present case study used cold water storage tank as shown in Figure 1.

The cylindrical tank has a 400 mm diameter and a 1000 mm height where it has equal-diameter 17.39 mm at inlet and outlet ports, while the baffles dimensions was 200 mm*2 mm length and thickness respectively. The tank was in a vertical position, the initial temperature of water in a tank is 4.4°C, and water enters from upper left side of the tank with temperature of

13.3°C. Constant inlet velocity and temperature are assumed during simulation. This study included four cases according to number of baffles in the tank as shown in Figure 2. Case 1 presents the study without baffles, case two with one baffle, case three with two baffles and case four with three baffles where the distance between each baffle equal to 0.25 m from the tank height.

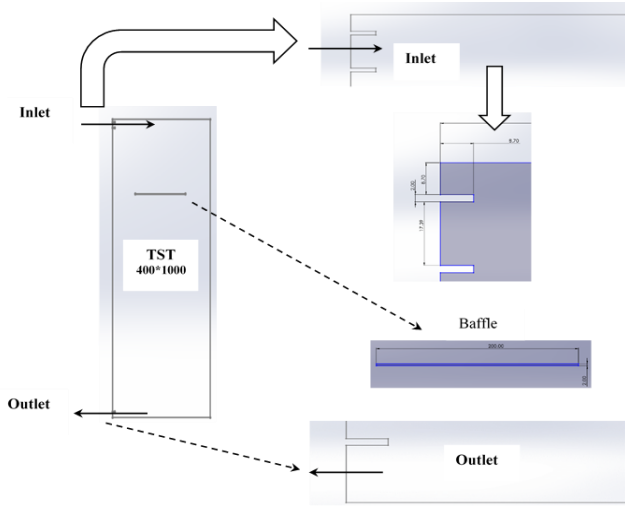


Figure 1. Dimensions of the present case study (mm)

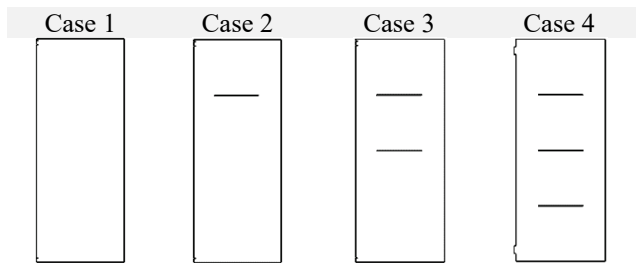


Figure 2. Case studies configuration

3. NUMERICAL SIMULATION

3.1 Governing equations

The governing equations of the current case study are the continuity, momentum and the energy equations. The

equations in this study are expressed as follows in 2D Cartesian coordinates.

The continuity equation:

$$\frac{\partial \rho}{\partial t} + \sum_{i=1}^2 \frac{\partial}{\partial x_i} (\rho u_i) = 0 \quad (1)$$

The momentum equation:

$$\frac{\partial (\rho u_i)}{\partial t} + \sum_{j=1}^2 \frac{\partial}{\partial x_j} (\rho u_j u_i) = -\frac{\partial P}{\partial x_i} + \sum_{j=1}^2 \frac{\partial \tau_{ij}}{\partial x_j} + \rho f_i \quad (2)$$

The energy equation:

$$\rho C_p \frac{\partial T}{\partial t} = \text{div}(\lambda \overrightarrow{\text{grad}} T) + T\beta \frac{\partial P}{\partial t} + q + \Phi \quad (3)$$

where,

$$\Phi = -\frac{2}{3} \mu (\text{div } \vec{u})^2 + 2\mu S_{ii} \frac{\partial u_i}{\partial x_j}$$

$$S_{ii} = \frac{1}{2} \left(\frac{\partial u_i}{\partial x_j} + \frac{\partial u_j}{\partial x_i} \right)$$

The assumptions for numerical solution are:

- Transient condition, two-dimensional incompressible flow with heat transfer inside the tank.
- Turbulent flow.
- Constant water properties.
- In water density modeling, boussinesq approximations are used, which means that, with the exception of linear density fluctuations in the buoyancy factor, water density is treated as a constant value in all solved equations.

$$\rho = \rho_o [1 - \beta(T - T_o)] \quad (4)$$

- For the examination of the transient behavior of thermal stratification, the standard k-ε turbulence model is employed, which includes full buoyancy effects and default turbulent constants.

3.2 Boundary conditions

Boundary conditions for inlet, outlet, baffles, tank walls and turbulence parameters are presented in Figure 3. Moreover, to initial condition and working fluid.

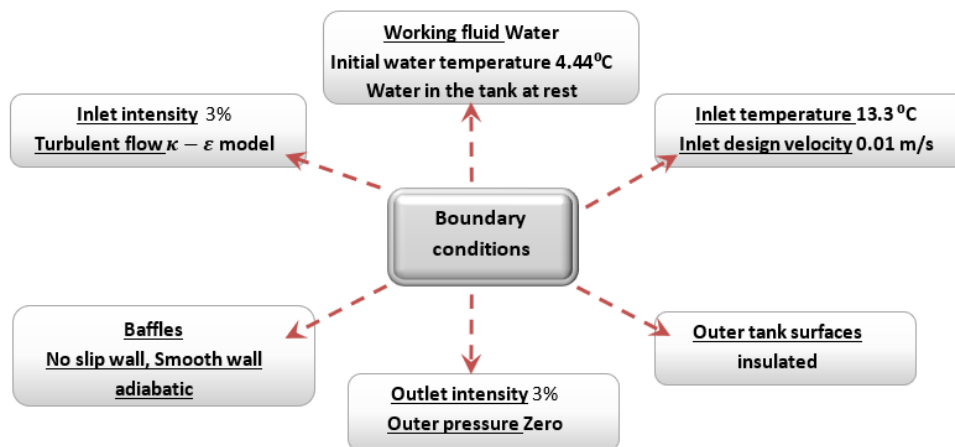


Figure 3. Boundary conditions details of physical models

3.3 Mesh generation and grid independency

Structured grids were utilized to build the physical model's grids. The grids were uniform. Number of nodes was 393620 while the number of elements was 392043. Where the mesh consists of 52,100 nodes and 48,819 hexahedron elements, as shown in Figure 4.

The grid independency test was carried out in order to discover a suitable result. structured grid is used in the computational domain and the solution is applied for the tank model with different grid size. In this study time step was 0.05 s and the average outlet temperature, Str no. were compared for different cases as shown Table 1. Where for both cell size 0.5 mm and 2 mm, differ from the cell size 1 mm insignificantly, and their maximum difference is 3.18%. Therefore, the solution with the cell size 1 mm was selected in this study.

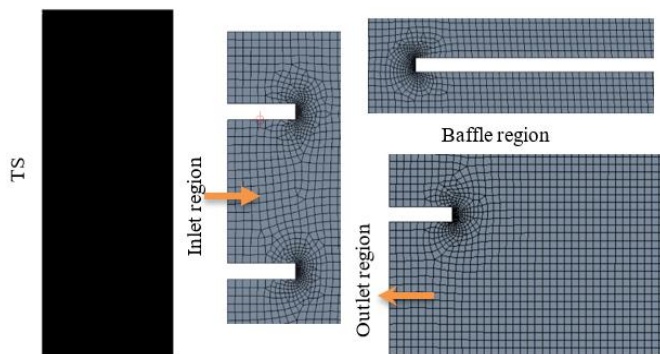


Figure 4. Structured grid for the tank domain

Table 1. Effect of different cell size on results parameters during Case 1

Element Size (mm)	0.5	1	2
Element No.	784,086	392043	196021
Discharge Time (min)	37.01	37.11	38.06
Str No.	0.066	0.062	0.068
Average Outlet Temperature °C	4.30	4.40	4.26
Error %	2.27	0	3.18

3.4 Validation test

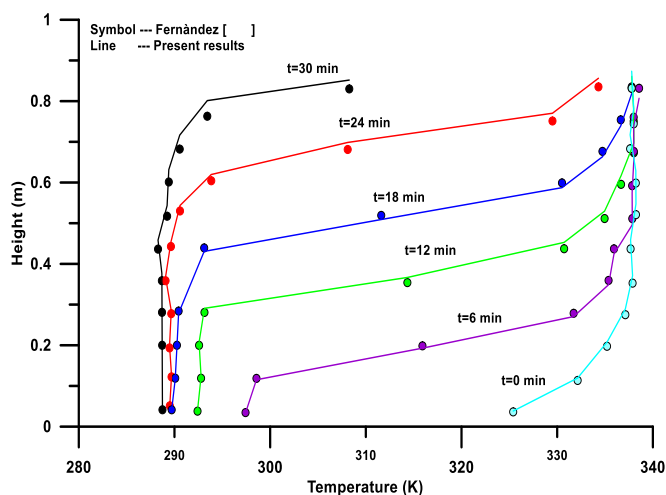


Figure 5. History of vertical temperature distribution in the tank with the results of the study [10]

It is frequently necessary to demonstrate the validity of the results from numerical simulations. As a result, validation experiments and simulations must include accounting for numerical and modeling errors. Present numerical simulations are carried out, and the results are compared between the experimental data by Abdelhak et al. [10] and current numerical results as shown in Figure 5. The results are statistically significant with a very high r-square value (above 0.95) [10].

4. RESULTS AND DISCUSSION

4.1 Baffles effect

Several factors have an impact on the temperature stratification inside the storage tank. As a result, the flowing section shows how baffles number and position effect on the temperature distribution, flow behavior inside the tank and the mixing shape during transient simulations. Four cases considered (Case 1 no baffle, Case 2 with one baffle added, Case 3 with two baffles added and Case 4 with four baffles added) the study considered the effect of baffle number for the time period of (100, 720, 1620, 2173) seconds and the results is shown in Figure 6 which shows the evolution of baffles number effect on temperature contours, streamlines, and velocity vector in the tank during transient operation for different baffles location in the tank.

During simulations the transient flow behavior, in particular the establishment of the thermocline and the related entrainment mechanisms were presented. When charging, a vortex is created close to the inlet port when the entering cold jet collides with the bottom layers. The cold water with heavy density falls down dragging simultaneously the upper-layer water into the bottom. The dragged-down filament rises and diffuses among the fluid layers as a result of the buoyancy effect, adding to the convection action. These imbalanced gravitational forces and inhomogeneous penetration help to improve mixing, which can affect the majority of the tank's volume. The thermocline region tends to move from the bottom of the tank to the top as time goes on, and the mixing zone gradually widens according to isotherms results. At $t=100$ s, the uniform zone occupies more than half of the tank while the stratified region at the top becomes significantly thinner, creating a well-mixed tank. This phenomenon is plainly visible for all flat plate position configurations. Considering the temperature contours, it is noted that the penetration of temperature gradient is nearly not affected by adding one and two baffles as we go from Case 1 to Case 3. While in Case 4, we note that although the penetration of temperature gradient with time remained of the same manner going from the top of the tank to the bottom, yet a wider cold-hot interaction region witnessed adding an effect on the temperature distribution up in the hot region and down in the cold region.

This occurred on time interval (100, 720, and 1620) seconds only while the temperature contours remained of the same pattern for Case 4 comparing with other cases in time interval till 2173 second. Also, the results showed that adding one baffle in Case 1 changed the formation of vortices inside the tank from one large vortex in (2173.4 seconds) examination into a formation of two small vortices near the inlet and the outlet zones. During the examined periods, a falling down of the vortex witnessed from region bellow the baffle down going to tank bottom as time passed.

Adding one more baffle each case up to Case 3 (of two baffles) eliminated the existence of the bottom vortex keeping the flow pattern nearly the same considering the time period (2173.4 seconds) this happened with temporary formation of vortex below the second baffle (from the top of the tank) yet it vanished as time passed. Also, in Case 4 also resulted in elimination of bottom vortex in the period (2173.4 seconds) but one more vortex occurred between the second and third baffle (counting from the top) in this time interval with wider top vortex formation. Observing the stream line formation during the studied periods for Case 3, we noticed more than

four vortices formation which eventually reduced into two final vortices.

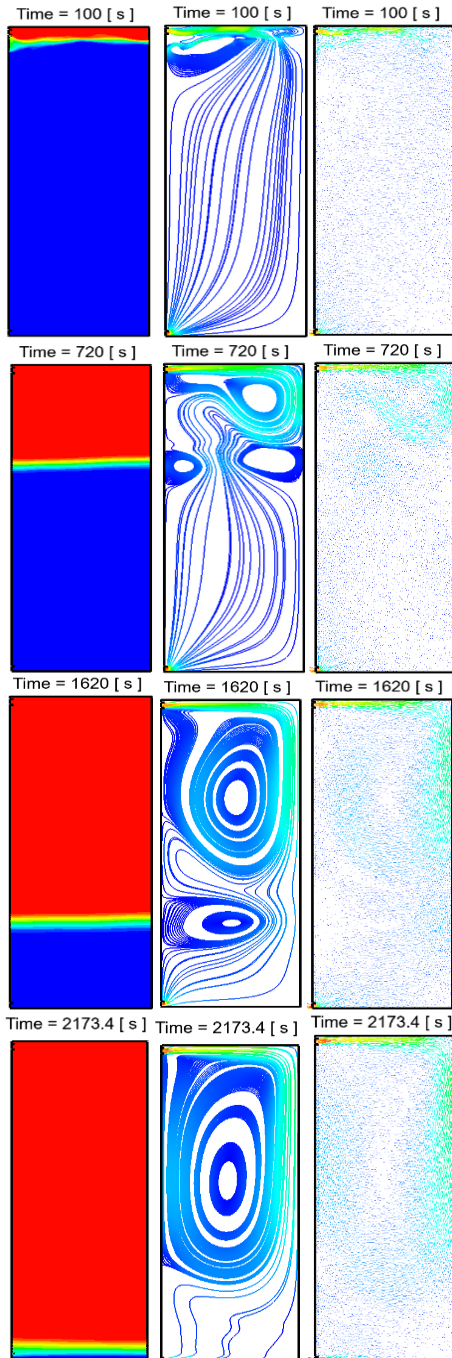
For the velocity vectors visualization, a less velocity values are shown by adding the first baffle in Case 2, the values of velocity vectors increased by adding the second baffle in Case 3 while it showed a rise in high velocity vector values of entrance up word, this is converted in the time periods of Case 4 while it returned to the same high entrance velocity rising up in the interval (2173.4 seconds) of Case 4 with more penetration of high velocity vectors down to the middle of the tank.

Temperature Contour

$T_h=13.3^{\circ}\text{C}$
 $T_c=4.4^{\circ}\text{C}$

Streamlines

Velocity Vector

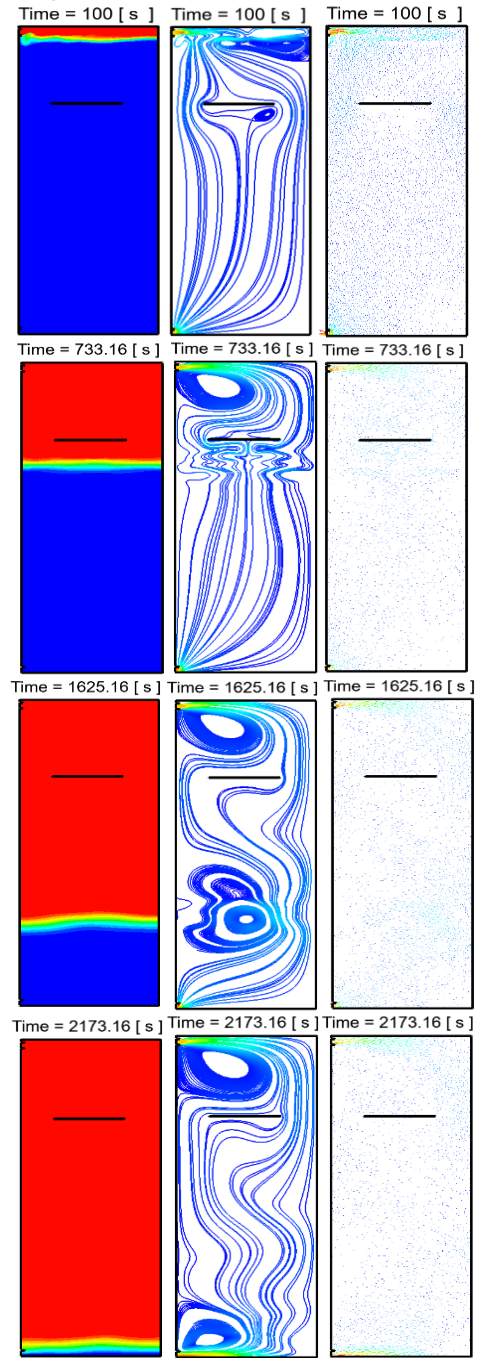


Temperature Contour

$T_h=13.3^{\circ}\text{C}$
 $T_c=4.4^{\circ}\text{C}$

Streamlines

Velocity Vector



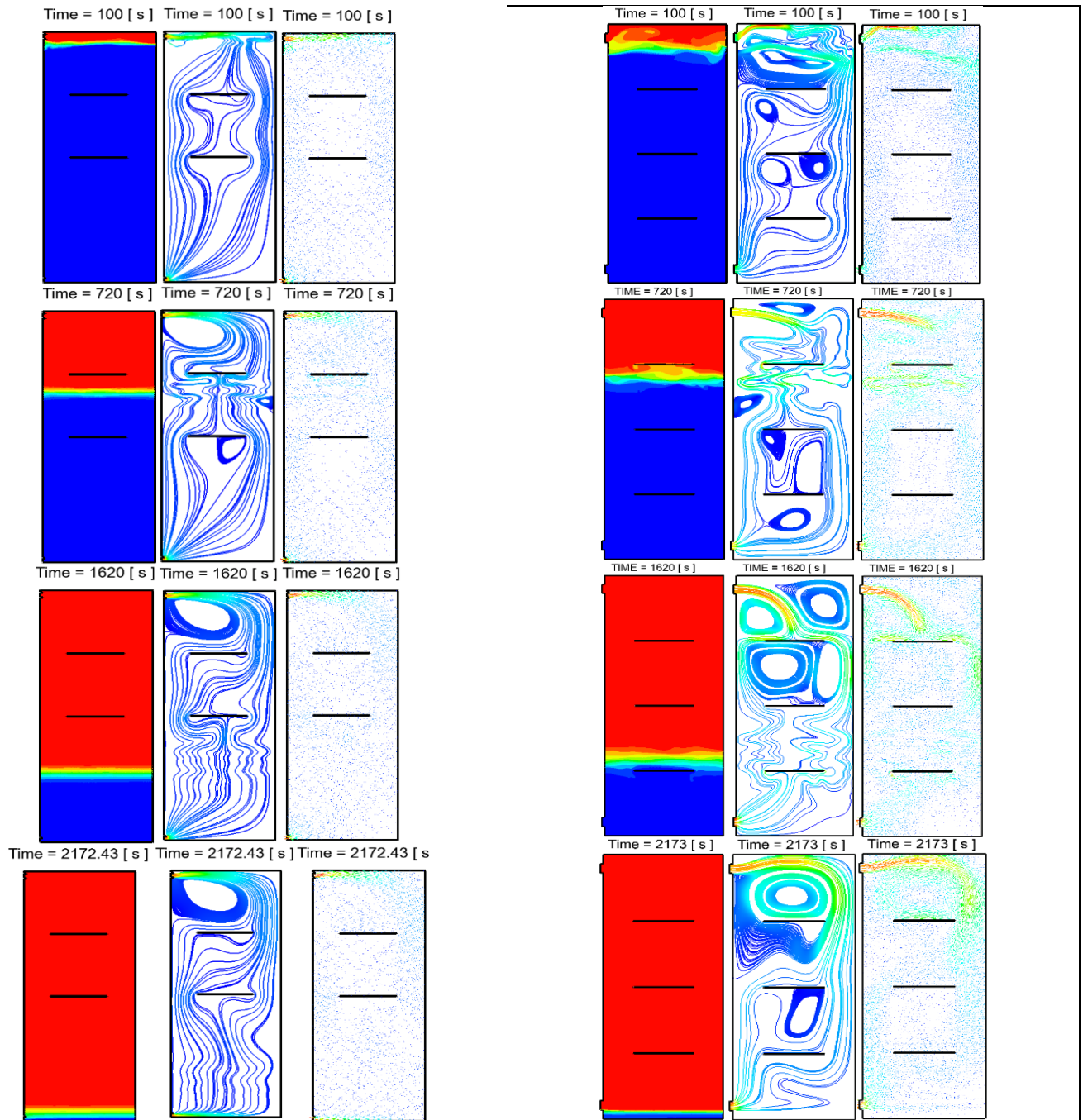
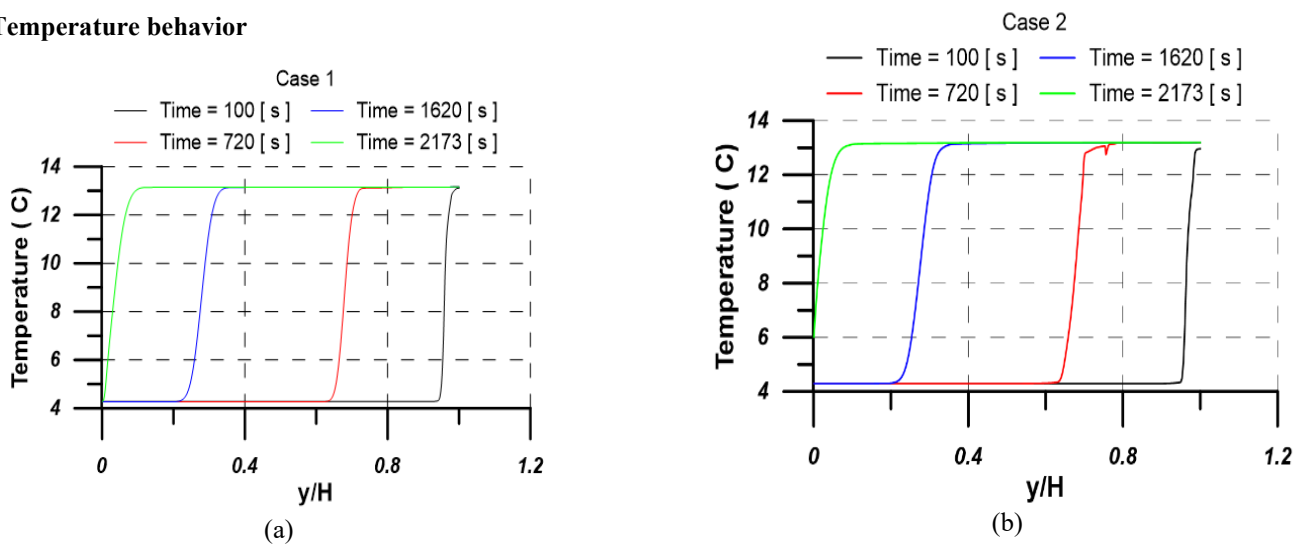


Figure 6. The effect of baffles number on temperature contours, streamlines, and velocity vector in the tank

4.2 Temperature behavior



$$(\partial T / \partial y)_{max} = \frac{T_{max} - T_{in}}{(J-1) \Delta y} \quad (7)$$

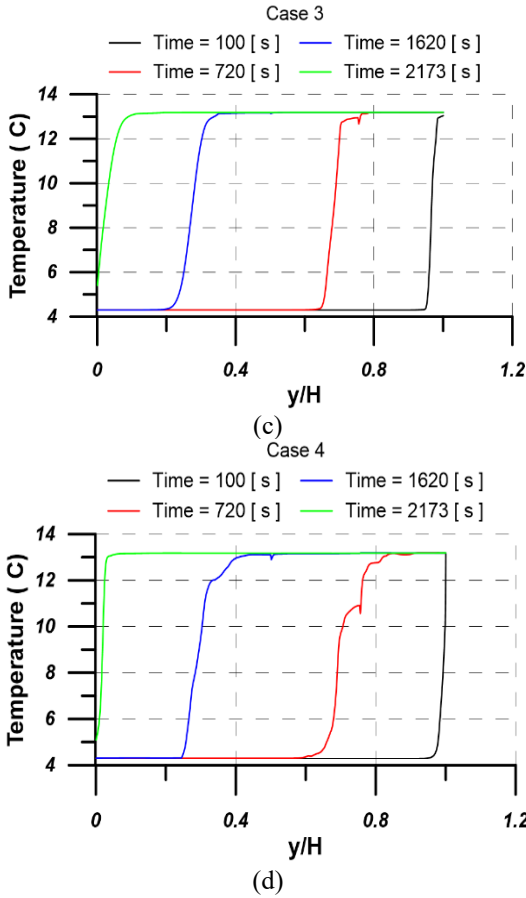


Figure 7. History of vertical temperature distribution in the tank

The history of temperature distribution over tank height for all cases are presented in Figure 7. The results applied in the centerline of the tank along vertical axes. In all cases the temperature distribution is uniform but there is a small difference in the distributions when the baffles exist as shown in case four. Where the baffles lead to the flow mixing inside the tank becomes small. As a result, the discharge mode with cold water become longer than the case without baffles. The results present the influence of injecting cold water at 4.44°C on the temperature behavior between time range from 0 s to 2173 s. The effect of different vertical positions on the dimensionless axis's.

4.3 Stratification number

A vertical storage tank's stratification can be described by a dimensional number called the stratification number [45, 46]. This crucial measure could assess the thermal behavior of the storage tank during the process of discharging. Consequently, to learn more specifically about how thermal stratification developed in both configurations under study, the stratification number calculated as the ratio of the greatest mean temperature gradient for the charging and discharging modes to the mean of the transient temperature gradients was used as expressed by Eq. (5):

$$Str(t) = \frac{\overline{(\partial T / \partial y)_t}}{(\partial T / \partial y)_{max}} \quad (5)$$

where,

$$\overline{(\partial T / \partial y)_t} = \frac{1}{J-1} \left[\sum_{j=1}^{J-1} \left(\frac{T_{j+1} - T_j}{\Delta y} \right) \right] \quad (6)$$

The tank's discharge takes 2173 seconds due to the flow that is applied during racking. Due to this, the evolution of the stratification number was evaluated throughout this time. In order to forecast how the position of the baffles will affect the degree of stratification inside the storage tank, the stratification number *Str* is determined during this study at the vertical centerline of the tank.

Figure 8 presents the evolution of the *Str* over a period of 2173 s for all cases. For the discharging operation, it is in our best interest to maintain a maximum lamination number in order to guarantee the ideal thermocline thickness. This indication is affected by the variance in local temperature along the vertical tank's axis and the minimum temperature of the water that will be charged. In comparison to the other configurations, the results show that increasing the number of baffles leads to higher thermocline performance, as demonstrated in Figure 4.

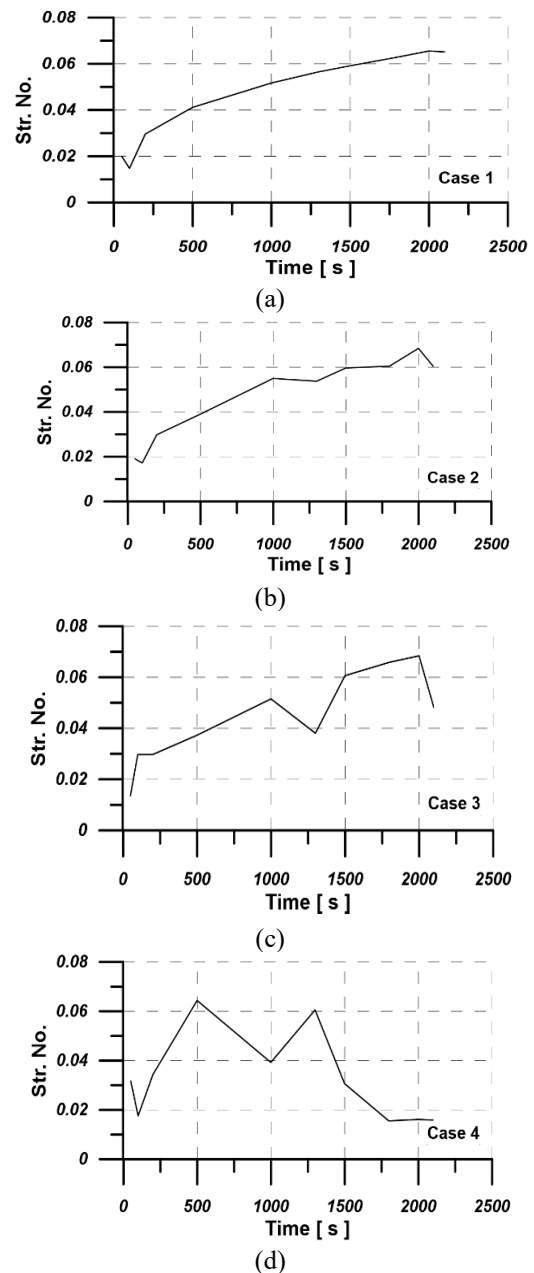


Figure 8. History of Stratification number in the tank for all cases

4.4 Richardson number

The stratification in hot water storage tanks is commonly described using the Richardson number, an important quantity that affects fluid flow [39, 40]. The Richardson number, which is represented as, measures the proportion of buoyancy forces to mixing forces.

$$Ri = \frac{\text{Buoyancy Force}}{\text{Inertial Force}} = \frac{g \cdot \beta \cdot H \cdot (T_{hot} - T_{cold})}{u_{in}^2} \quad (18)$$

As can be observed, $Ri > 1$ might experience a positive thermal stratification. Figure 9 illustrates the Richardson number's development for four cases as discharging progressed. As observed, the Richardson number is fluctuations during discharge period time. This can be explained by the fact that mixing forces have an impact on the tank's flow pattern. Due to the presence of two recirculation zones in baffle cases, mixing forces are more apparent.

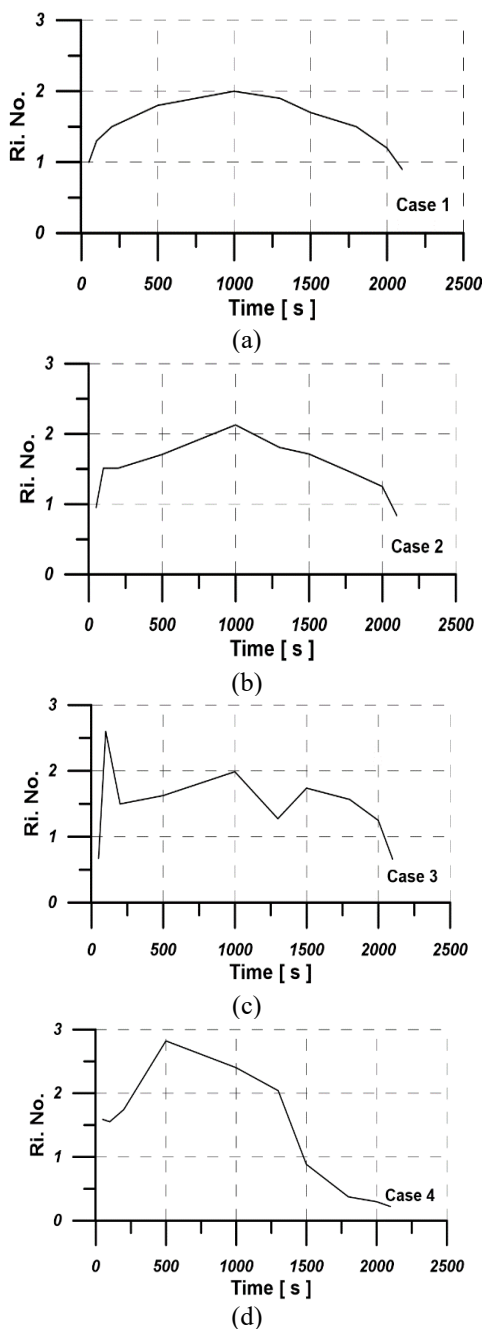


Figure 9. History of Richardson number in the tank for different cases

5. CONCLUSION

The simulation results reveal the behavior of the fluid and temperature distribution within the tank. The incorporation of one or two baffles had a marginal impact on the temperature distribution contours. However, the addition of a third baffle significantly influenced the temperature distribution contours, as the hot-cold interface expanded with more significant penetration effects in both the cold and hot regions. Generally, the impact of adding three baffles on temperature distribution contours dissipated at the discharging time (2173.4 seconds).

Regarding the influence of baffle addition on the streamlines within the tank, a more defined streamline was established in the time interval (2173.4 seconds). The final streamline formation achieved by adding two baffles yielded better results compared to the addition of three baffles. Nevertheless, incorporating a third baffle enhanced the final streamline formation compared to the no-baffle scenario (case1). This occurred alongside changes in flow characteristics within the tank, with alterations in vortex formation observed as the creation of a single large vortex was eliminated when the tank discharge time was reached. The addition of a single baffle reduced the calculated values of the velocity vectors, while the incorporation of a second baffle moderately increased them. The inclusion of a third baffle further amplified the velocity vectors, with a higher velocity gradient penetrating down to the mid-section of the tank.

The increment in the number of baffles led to improvements in the thermocline, as observed in the studied cases. More mixing forces were also evident due to the presence of two recirculating zones.

REFERENCES

- [1] Yaici, W., Ghorab, M., Entchev, E., Hayden, S. (2013). Three-dimensional unsteady CFD simulations of a thermal storage tank performance for optimum design. *Applied Thermal Engineering*, 60(1-2): 152-163. <https://doi.org/10.1016/j.applthermaleng.2013.07.001>
- [2] Chung, J.D., Cho, S.H., Tae, C.S., Yoo, H. (2008). The effect of diffuser configuration on thermal stratification in a rectangular storage tank. *Renewable Energy*, 33(10): 2236-2245. <https://doi.org/10.1016/j.renene.2007.12.013>
- [3] Mawire, A., McPherson, M., Van den Heetkamp, R.R.J., Mlatho, S.J.P. (2009). Simulated performance of storage materials for pebble bed thermal energy storage (TES) systems. *Applied Energy*, 86(7-8): 1246-1252. <https://doi.org/10.1016/j.apenergy.2008.09.009>
- [4] Baik, Y.J., Kim, M., Cho, J., Ra, H.S., Lee, Y.S., Chang, K.C. (2014). Performance variation of the TEES according to the changes in cold-side storage temperature. *International Journal of Mechanical and Mechatronics Engineering*, 8(8): 1413-1416. <https://doi.org/10.5281/zenodo.1094249>
- [5] Al-Maliki, W.A.K., Mahmoud, N.S., Al-Khafaji, H.M., Alobaid, F., Epple, B. (2021). Design and implementation of the solar field and thermal storage system controllers for a parabolic trough solar power plant. *Applied Sciences*, 11(13): 6155. <https://doi.org/10.3390/app11136155>
- [6] Chaichan, M.T., Kazem, H.A. (2011). Thermal storage comparison for variable basement kinds of a solar

- chimney prototype in Baghdad-Iraq weathers. *International journal of Applied Science (IJAS)*, 2(2): 12-20.
- [7] Raccanello, J., Rech, S., Lazzaretto, A. (2019). Simplified dynamic modeling of single-tank thermal energy storage systems. *Energy*, 182: 1154-1172. <https://doi.org/10.1016/j.energy.2019.06.088>
- [8] Suresh, C., Saini, R.P. (2020). Review on solar thermal energy storage technologies and their geometrical configurations. *International Journal of Energy Research*, 44(6): 4163-4195. <https://doi.org/10.1002/er.5143>
- [9] Alva, G., Lin, Y., Fang, G. (2018). An overview of thermal energy storage systems. *Energy*, 144: 341-378. <https://doi.org/10.1016/j.energy.2017.12.037>
- [10] Abdelhak, O., Mhiri, H., Bournot, P. (2015). CFD analysis of thermal stratification in domestic hot water storage tank during dynamic mode. *Building Simulation*, 8: 421-429. <https://doi.org/10.1007/s12273-015-0216-9>
- [11] Kong, L., Zhu, N. (2016). CFD simulations of thermal stratification heat storage water tank with an inside cylinder with openings. *Procedia Engineering*, 146: 394-399. <https://doi.org/10.1016/j.proeng.2016.06.419>
- [12] Fan, J., Furbo, S. (2012). Thermal stratification in a hot water tank established by heat loss from the tank. *Solar Energy*, 86(11): 3460-3469. <https://doi.org/10.1016/j.solener.2012.07.026>
- [13] Han, Y.M., Wang, R.Z., Dai, Y.J. (2009). Thermal stratification within the water tank. *Renewable and Sustainable Energy Reviews*, 13(5): 1014-1026. <https://doi.org/10.1016/j.rser.2008.03.001>
- [14] Wilk, J., Bałon, P., Smusz, R., Rejman, E., Świątoniowski, A., Kielbasa, B., Szostak, J., Cieślak, J., Kowalski, Ł. (2020). Thermal stratification in the storage tank. *Procedia Manufacturing*, 47: 998-1003. <https://doi.org/10.1016/j.promfg.2020.04.306>
- [15] Gómez, M.A., Collazo, J., Porteiro, J., Míguez, J.L. (2018). Numerical study of an external device for the improvement of the thermal stratification in hot water storage tanks. *Applied Thermal Engineering*, 144: 996-1009. <https://doi.org/10.1016/j.applthermaleng.2018.09.023>
- [16] Bouhal, T., Fertahi, S., Agrouaz, Y., El Rhafiki, T., Kousksou, T., Jamil, A. (2017). Numerical modeling and optimization of thermal stratification in solar hot water storage tanks for domestic applications: CFD study. *Solar Energy*, 157: 441-455. <https://doi.org/10.1016/j.solener.2017.08.061>
- [17] Shaarawy, M., Lightstone, M. (2016). Numerical analysis of thermal stratification in large horizontal thermal energy storage tanks. *Journal of Solar Energy Engineering*, 138(2): 021009. <https://doi.org/10.1115/1.4032451>
- [18] Penkova, N., Harryzanov, N. (2014). Analysis and optimization of temperature stratification in a thermal energy storage tank. In *Proceedings at 5th International Conference on Energy and Sustainability*, pp. 469-477. <https://doi.org/10.2495/esus140401>
- [19] Tesfay, M., Venkatesan, M. (2013). Simulation of thermocline thermal energy storage system using C. *International Journal of Innovation and Applied Studies*, 3(2): 354-364.
- [20] Shaikh, W., Wadegaonkar, A., Kedare, S.B., Bose, M. (2018). Numerical simulation of single media thermocline based storage system. *Solar Energy*, 174: 207-217. <https://doi.org/10.1016/j.solener.2018.08.084>
- [21] Aljabair, S., Alesbe, I., Ibrahim, S.H. (2021). Review on latent thermal energy storage using phase change material. *Journal of Thermal Engineering*, 9(1): 247-256. <https://doi.org/10.18186/thermal.1245298>
- [22] Njoku, H.O., Ekechukwu, O.V., Onyegegbu, S.O. (2014). Analysis of stratified thermal storage systems: An overview. *Heat and Mass Transfer*, 50: 1017-1030. <https://doi.org/10.1007/s00231-014-1302-8>
- [23] Mao, Q. (2016). Recent developments in geometrical configurations of thermal energy storage for concentrating solar power plant. *Renewable and Sustainable Energy Reviews*, 59: 320-327. <https://doi.org/10.1016/j.rser.2015.12.355>
- [24] Baghel, S., Shinde, S. (2017). CFD analysis of non-linear sloshing in a cylindrical tank. *International Journal of Research in Engineering and Technology*, 6(12): 118-122. <https://doi.org/10.15623/ijret.2017.0612018>
- [25] Li, A., Cao, F., Zhang, W., Shi, B., Li, H. (2018). Effects of different thermal storage tank structures on temperature stratification and thermal efficiency during charging. *Solar Energy*, 173: 882-892. <https://doi.org/10.1016/j.solener.2018.08.025>
- [26] Gao, L., Lu, H., Sun, B., Che, D., Dong, L. (2021). Numerical and experimental investigation on thermal stratification characteristics affected by the baffle plate in thermal storage tank. *Journal of Energy Storage*, 34: 102117. <https://doi.org/10.1016/j.est.2020.102117>
- [27] Saghi, H., Lakzian, E. (2017). Optimization of the rectangular storage tanks for the sloshing phenomena based on the entropy generation minimization. *Energy*, 128: 564-574. <https://doi.org/10.1016/j.energy.2017.04.075>
- [28] Saghi, H. (2016). The pressure distribution on the rectangular and trapezoidal storage tanks' perimeters due to liquid sloshing phenomenon. *International Journal of Naval Architecture and Ocean Engineering*, 8(2): 153-168. <https://doi.org/10.1016/j.ijnaoe.2015.12.001>
- [29] Thirunavukkarasu, B., Rajagopal, T.K.R. (2022). Numerical investigation of sloshing in a three-dimensional square tank under excitation using CFD code. *Ships and Offshore Structures*, 17(2): 304-318. <https://doi.org/10.1080/17445302.2020.1827640>
- [30] Sanapala, V.S., Rajkumar, M., Velusamy, K., Patnaik, B.S.V. (2018). Numerical simulation of parametric liquid sloshing in a horizontally baffled rectangular container. *Journal of Fluids and Structures*, 76: 229-250. <https://doi.org/10.1016/j.jfluidstructs.2017.10.001>
- [31] Boetcher, S.K., Kulacki, F.A., Davidson, J.H. (2012). Use of a shroud and baffle to improve natural convection to immersed heat exchangers. *Journal of Solar Energy Engineering*, 134(1): 011010. <https://doi.org/10.1115/1.4005089>
- [32] Hamza, N.F., Aljabair, S. (2023). Numerical and experimental investigation of heat transfer enhancement by hybrid nanofluid and twisted tape. *Engineering and Technology Journal*, 41(1): 69-85. <https://doi.org/10.30684/ETJ.2022.131909.1069>
- [33] Hamza, N.F.A., Aljabair, S. (2022). Evaluation of thermal performance factor by hybrid nanofluid and twisted tape inserts in heat exchanger. *Heliyon*, 8(12). <https://doi.org/10.1016/j.heliyon.2022.e11950>
- [34] Goudarzi, M.A., Sabbagh-Yazdi, S.R., Marx, W. (2010). Investigation of sloshing damping in baffled rectangular

- tanks subjected to the dynamic excitation. *Bulletin of Earthquake Engineering*, 8: 1055-1072. <https://doi.org/10.1007/s10518-009-9168-8>
- [35] Beemkumar, N., Karthikeyan, A., Reddy, K.S.K., Rajesh, K., Anderson, A. (2017). Analysis of thermal energy storage tank by ANSYS and comparison with experimental results to improve its thermal efficiency. *IOP Conference Series: Materials Science and Engineering*, 197(1): 012039. <https://doi.org/10.1088/1757-899x/197/1/012039>
- [36] Li, H., Sun, H., Feng, G. (2017). Numerical simulation analysis of heat storage and release performance in baffle plate phase change energy storage tank. *Procedia Engineering*, 205: 3334-3339. <https://doi.org/10.1016/j.proeng.2017.10.362>
- [37] Gedikli, A., Ergüven, M.E. (1999). Seismic analysis of a liquid storage tank with a baffle. *Journal of Sound and Vibration*, 223(1): 141-155. <https://doi.org/10.1006/jsvi.1999.2091>
- [38] Gualtieri, C. (2009). Analysis of flow and concentration fields in a baffled circular storage tank. 33rd IAHR Congress: Water Engineering for a Sustainable Environment, pp. 4384-4392.
- [39] Habeeb, A.S., Karamallah, A.A., Aljabair, S. (2022). Review of computational multi-phase approaches of nano-fluids filled systems. *Thermal Science and Engineering Progress*, 28: 101175. <https://doi.org/10.1016/j.tsep.2021.101175>
- [40] Habeeb, A.S., Aljabair, S., Karamallah, A.A. (2022). Experimental and numerical assessment on hydrothermal behaviour of MgO-Fe₃O₄/H₂O hybrid nano-fluid. *International Journal of Thermofluids*, 16: 100231. <https://doi.org/10.1016/j.ijft.2022.100231>
- [41] S Habeeb, A., Aljabair, S., Karamallah, A.A. (2023). Computational single and multiphase approaches to investigate the hydrothermal behavior of hybrid nano-fluid in plain and wavy tubes. *Engineering and Technology Journal*, 41(7): 1-19. <https://doi.org/10.30684/ETJ.2023.136449.1316>
- [42] Hashim, A.A.A., Abdulrasool, A.A. (2019). Numerical verification for different types of curved baffles as stratifiers in solar thermal storage tank. *IOP Conference Series: Materials Science and Engineering*, 518(3): 032052. <https://doi.org/10.1088/1757-899x/518/3/032052>
- [43] Gao, H., Stenstrom, M.K. (2019). Generalizing the effects of the baffling structures on the buoyancy-induced turbulence in secondary settling tanks with eleven different geometries using CFD models. *Chemical Engineering Research and Design*, 143: 215-225. <https://doi.org/10.1016/j.cherd.2019.01.015>
- [44] Alesbe, I., Wahhab, H.A.A., Aljabair, S. (2023). Transient study of thermal stratification of full-scale chilled water storage tank during optimum discharge condition. *Journal of Energy Storage*, 65: 107236. <https://doi.org/10.1016/j.est.2023.107236>
- [45] Fernandez-Seara, J., Uhi, F.J., Sieres, J. (2007). Experimental analysis of a domestic electric hot water storage tank. Part II: Dynamic mode of operation. *Applied Thermal Engineering*, 27(1): 137-144. <https://doi.org/10.1016/j.applthermaleng.2006.05.004>
- [46] Fernández-Seara, J., Uhía, F.J., Sieres, J. (2007). Experimental analysis of a domestic electric hot water storage tank. Part I: Static mode of operation, *Applied Thermal Engineering*, 27(1): 129-136. <https://doi.org/10.1016/j.applthermaleng.2006.05.006>

NOMENCLATURE

<i>CFD</i>	Computational Fluid Dynamics [-]
C_p	Specific heat [kJ/kg-K]
f_i	Body force [N/kg]
g	Gravitational acceleration [m/s ²]
H	Tank height [m]
h	Diffuser height [m]
<i>Str</i>	Stratification number
P	Static pressure [Pa]
q	Source term [J/(s·m ³)]
Ri	Richardson number [-]
r	Radius of pipe inlet [m]
T	Temperature [°C]
<i>TST</i>	Thermal storage tank [-]
t	Time [s]
u	Water velocity [m/s]
x	Cartesian coordinates [m]

Greek symbols

ρ	Density, [kg/m ³]
β	Coefficient of thermal expansion (K ⁻¹)
λ	Thermal diffusivity [m ² /s]
μ	Dynamic viscosity [Pa.s]
τ_{ij}	Viscous stress [N/m ²]
Δt	Time step [s]
Δx	Cell size [m]

Subscripts

<i>ini, o</i>	Initial condition
<i>in, out</i>	Inlet and outlet conditions
<i>st</i>	Stratification condition